PROCEEDINGS OF SCIENCE

Hunting scalar partners of the Higgs boson at the LHC

Werner Porod*

Institut für Theoretische Physik und Astrophysik, Uni Würzburg, Emil-Hilb-Weg 22, D-97074 Würzburg, Germany

E-mail: porod@physik.uni-wuerzburg.de

Composite Higgs models with a fermionic ultraviolet completion predict in general additional pseudo Nambu Goldstone bosons beside the Higgs multiplet. In this contribution we discuss their LHC signatures and present first bounds in simplified models which can also be applied to generic models like multi-Higgs models. We then demonstrate how these can be combined taking a concrete model based on the SU(5)/SO(5) coset as an example. We use this to show how a proper combination of different channels can lead to an improved bound compared to a single channel analysis.

Corfu Summer Institute 2022 "School and Workshops on Elementary Particle Physics and Gravity",
28 August - 1 October, 2022
Corfu, Greece

*Speaker

https://pos.sissa.it/

PoS(CORFU2022)126

1. Introduction

The Standard Model (SM) of particle physics features a single scalar field being a doublet of weak isospin $\mathrm{SU}(2)_L$ that is responsible for the breaking of the electroweak (EW) symmetry [1, 2]. Once it acquires a vacuum expectation value (vev), a massive physical scalar particle arises, the Higgs boson [2] discovered in 2012 at the Large Hadron Collider (LHC) experiments [3, 4]. In contrast, most models of new physics contain extended Higgs sectors: for instance, minimal supersymmetric models [5] and two Higgs doublet models [6] feature a second doublet and the type-II seesaw models [7, 8] a zero hypercharge triplet. Scalar triplets appear also in the Georgi-Machacek model [9]. In all these scenarios, the scalar fields acquire sizeable couplings to the SM gauge bosons and fermions via vevs and/or via mixing with the SM Higgs boson. Consequently, they are dominantly singly-produced at colliders, and most current searches focus on these channels.

Single production of a scalar is always model dependent and it can be suppressed by tuning the single-scalar couplings. By contrast, pair production only depends on the gauge quantum numbers of the scalars and cannot be tuned to be small. The couplings of two scalars from $\mathrm{SU}(2)_L \times \mathrm{U}(1)_Y$ multiplets to the EW gauge bosons stem from the covariant derivatives in the scalar kinetic terms and are always present. Their presence imply dominant pair production channels via Drell-Yan processes, where two initial state quarks merge via an s-channel gauge boson. There is some model dependence if their is mixing in the scalar sector but this mixing cannot reduce Drell-Yan pair production cross sections of all scalars at the same time and some channels are guaranteed to remain sizeable.

In this contribution, we focus on models where pair production is the dominant mode for scalars charged under $\mathrm{SU}(2)_L \times \mathrm{U}(1)_Y$. Such scenarios appear naturally in composite Higgs models, where the Higgs boson is accompanied by additional light states, protected by parities internal to the strong sector [10]. The Higgs boson emerges in these models as a pseudo-Nambu-Goldstone boson (pNGB) [11] following the dynamical breaking of the EW symmetry triggered by misalignment in a condensing strong dynamics at the TeV scale [12, 13]. A minimal model $\mathrm{SO}(5)/\mathrm{SO}(4)$ based only on the global symmetries with exactly four pNGBs matching the Higgs doublet components can be constructed [14]. However, it is not easy to obtain this symmetry pattern in an underlying gauge/fermion theory *à la* QCD. A fermion condensate $\langle\psi\psi\rangle$ can only generate the following patterns [15, 16]: $\mathrm{SU}(2N)/\mathrm{Sp}(2N)$, $\mathrm{SU}(N)/\mathrm{SO}(N)$ or $\mathrm{SU}(N)^2/\mathrm{SU}(N)$ depending on whether the representation of ψ under the confining gauge symmetry is pseudo-real, real or complex, respectively. The minimal model with custodial symmetry [17, 18] features $\mathrm{SU}(4)/\mathrm{Sp}(4)$ [19, 20], and has one additional gauge singlet pNGB besides the Higgs doublet. The next-to-minimal cases contain significantly more pNGBs: 14 for $\mathrm{SU}(5)/\mathrm{SO}(5)$ [21, 22] and 15 for $\mathrm{SU}(4)^2/\mathrm{SU}(4)$ [23, 24]. The departure from minimality does not contradict the null results of direct searches for physics beyond the SM (BSM) at colliders. The pNGBs are typically heavier than the Higgs boson and have only EW interactions, hence being difficult to discover at hadron colliders and are too heavy for past e^+e^- colliders such as LEP or SLC.

The dominant channel is pair production via Drell-Yan and the vector boson fusion (VBF) pair production via gauge couplings is found to be subleading to Drell-Yan [25, 26]. VBF single production is generated via topological anomalies, hence it is suppressed by a small anomaly coupling. Drell-Yan single production could also be present if the pNGBs couple to quarks. However,

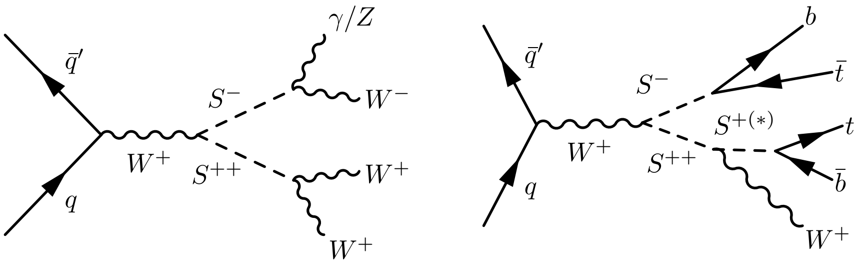

Figure 1: Examples of di-scalar channels from pair production via Drell-Yan processes with subsequent decays into SM particles.

it is expected that pNGBs in models with partial compositeness couple only very weakly to light quark flavours as the couplings are roughly proportional to the quark mass. Consequently, the dominant couplings involve third generation quarks and the neutral pNGBs can be singly-produced via gluon fusion similar to the Higgs boson. Moreover, both neutral and charged pNGBs can be singly-produced in association with either tt or tb. This can provide a relevant contribution if the couplings are large enough.

We will present here recent results from recent investigations presented in refs. [26, 27] to which we refer for further details. We will first discuss simplified models and then focus on a specific model based on SU(5)/SO(5) to present the interplay between various channels. This class of models can be realised in the context of four-dimensional models with a microscopic description [28–30] and emerges as the minimal symmetry pattern from the condensate $\langle\psi\psi\rangle$ of two EW-charged fermions if ψ is in a real irreducible representation of the confining gauge group, e.g. $Sp(4)$. We note for completeness, that the properties of the confining gauge dynamics, based on Sp(4), has been studied on the Lattice with promising results [31–34]. Complementary information on the mass spectrum and decay constants of the composite states can also be obtained using holographic techniques [35–37].

2. Bounds on Drell-Yan pair-produced scalars in simplified models

We start with bounds in simplified models where we focus on pair production, via the dominant Drell-Yan channels. We use parts of a simplified model which has been introduced in refs. [26, 27] to which we refer for the underlying Lagrangian. We extend the SM by colourless scalar states $S^0, S^{0\prime}, S^\pm, S^{\pm\pm}$ that are physical mass eigenstates labelled by their electric charge. We include the minimal set of states with charge up to two that have all the possible couplings to the EW gauge bosons. In case of the neutral we include two neutral states with opposite parity and assume that none of the BSM scalars obtains a non-zero vev.

We investigate all combinations of scalar pairs produced at the LHC through the Drell-Yan processes:

$$pp \to S^{\pm\pm}S^{\mp}\,,\; S^{\pm}S^{0(\prime)}\,,\; S^{++}S^{--}\,,\; S^{+}S^{-}\,,\; S^{0}S^{0\prime}\,. \tag{1}$$

Together with the first tier decays of the scalar pairs into SM particles, these production processes yield many di-scalar channels, see for example Fig. 1. Charge-conjugated states belong to the same channel. We consider two complementary scenarios for the decays of the scalars

fermiophobic	$S^{++}S^{--}$	$S^{\pm\pm}S^{\mp}$	$S^{+}S^{-}$	$S^{\pm}S^{0(\prime)}$	$S^{0}S^{0\prime}/S^{0\prime}S^{0}$
$WWWW$	$W^+W^+W^-W^-$	-	-	-	$W^+W^-W^+W^-$
$WWW\gamma$	-	$W^\pm W^\pm W^\mp\gamma$	-	$W^\pm\gamma W^+W^-$	-
$WWWZ$	-	$W^\pm W^\pm W^\mp Z$	-	$W^\pm ZW^+W^-$	-
$WW\gamma\gamma$	-	-	$W^+\gamma W^-\gamma$	-	$W^+W^-\gamma\gamma$
$WWZ\gamma$	-	-	$W^\pm\gamma W^\mp Z$	-	$W^+W^-\gamma Z$
$WWZZ$	-	-	W^+ZW^-Z	-	W^+W^-ZZ
$W\gamma\gamma\gamma$	-	-	-	$W^\pm\gamma\gamma\gamma$	-
$WZ\gamma\gamma$	-	-	-	$W^\pm\{Z\gamma\}\gamma$	-
$WZZ\gamma$	-	-	-	$W^\pm\{Z\gamma\}Z$	-
$WZZZ$	-	-	-	$W^\pm ZZZ$	-
$\gamma\gamma\gamma\gamma$	-	-	-	-	$\gamma\gamma\gamma\gamma$
$Z\gamma\gamma\gamma$	-	-	-	-	$Z\gamma\gamma\gamma$
$ZZ\gamma\gamma$	-	-	-	-	$Z\{Z\gamma\}\gamma$
$ZZZ\gamma$	-	-	-	-	$ZZZ\gamma$
$ZZZZ$	-	-	-	-	$ZZZZ$

Table 1: Classification of the 24 di-scalar channels in terms of the 5 pair production cases (columns) and the 15 combinations of gauge bosons (rows) from decays. In the channels, the first two and second two bosons are resonantly produced. The notation $\{Z\gamma\} = Z\gamma + \gamma Z$ indicates the two permutations. Charge-conjugated states belong to the same di-scalar channel.

1. The fermiophobic case, where couplings to SM fermions are absent at leading order and the dominant decays are into EW gauge bosons:

$$S^{++} \to W^+W^+\,, \tag{2a}$$
$$S^{+} \to W^+\gamma,\ W^+Z\,, \tag{2b}$$
$$S^{0(\prime)} \to W^+W^-,\ \gamma\gamma,\ \gamma Z,\ ZZ. \tag{2c}$$

   Combining the different Drell-Yan scalar pairs with the above decay channels leads to 24 di-scalar channels, each containing four gauge bosons. One sample process is shown in the left diagram of Fig. 1, while a complete list of all channels is shown in Table 1.

2. The fermiophilic case, where the scalars decay dominantly into a pair of third generation quarks:

$$S^{++} \to W^+ t\bar{b}, \tag{3a}$$
$$S^{+} \to t\bar{b}, \tag{3b}$$
$$S^{0(\prime)} \to t\bar{t} \quad \text{or} \quad b\bar{b}. \tag{3c}$$

   Note that doubly charged scalars cannot decay to two quarks due to their charge, but if they are part of an $\mathrm{SU}(2)_L$ multiplet, the three-body decay $S^{++} \to W^+S^{+*} \to W^+t\bar{b}$ is allowed. Consequently, this yields 8 possible di-scalar channels for pair-produced scalars in this scenario. One sample process is shown in the right diagram of Fig. 1 and a complete list in Tab. 2.

For the simulation of signal events we use the publicly available eVLQ model presented in ref. [26], which implements the simplified models as a FeynRules [38] model at next-to-leading

fermiophilic	$S^{++}S^{--}$	$S^{++}S^{-}$	$S^{+}S^{-}$	$S^{+}S^{0(\prime)}$	$S^{0}S^{0\prime}/S^{0\prime}S^{0}$
$tttt$	-	-	-	-	$t\bar{t}t\bar{t}$
$tttb$	-	-	-	$t\bar{b}t\bar{t}$	-
$ttbb$	-	-	$t\bar{b}b\bar{t}$	-	$t\bar{t}b\bar{b}$
$tbbb$	-	-	-	$t\bar{b}b\bar{b}$	-
$bbbb$	-	-	-	-	$b\bar{b}b\bar{b}$
$Wttbb$	-	$W^{+}t\bar{b}b\bar{t}$	-	-	-
$WWttbb$	$W^{+}t\bar{b}W^{-}b\bar{t}$	-	-	-	-

Table 2: Classification of the 8 di-scalar channels in terms of the 5 pair production cases (columns) and the 5 combinations of top and bottom from decays (rows). In cases with one or two doubly charged scalars, one always obtains $ttbb$ with one or two additional W's, respectively. The charge-conjugated states are not shown.

order in QCD. All events are generated at a centre-of-mass energy of 13 TeV in pp collisions. For each di-scalar channel, we perform a scan over the scalar mass m_S; for channels involving two different scalars, we assume them to be mass degenerate. We generate 10^5 events of Drell-Yan scalar pairs with decay into the target channel for each scan point. We use MadGraph5_aMC@NLO [39] version 3.3.2 at NLO, in association with the parton densities in the NNPDF 2.3 set [40, 41]. Afterwards, we interface the events with Pythia8 [42] for the decays of the SM particles, showering and hadronisation. The resulting signal events are then analysed with MadAnalysis5 [43–46] version 1.9.60 and CheckMATE [47, 48] version 2.0.34. Both tools reconstruct the events using Delphes 3 [49] and the anti-k_T algorithm [50] implemented in FastJet [51]. The exclusion associated with the events is calculated with the CL$_s$ prescription [52]. Moreover, we run the events against the SM measurements implemented in Rivet [53] version 3.1.5 and extract exclusions from the respective YODA files using Contur [54, 55] version 2.2.1. To present simplified model bounds, we determine the signal cross section σ_{95} which is excluded at 95% CL. We note for completeness, that the procedure differs somewhat between the tools and we refer to ref. [27] for the details. For each channel and each parameter point, we take the minimal value for σ_{95} obtained from MadAnalysis5, CheckMATE, and Contur as the final bound. We do not attempt to combine them.

We display results in Fig. 2, where we present the simplified model bounds on the cross section for various di-scalar channels, i.e. bounds on the production cross section of the scalar pair times both branching ratios. We show in Fig. 2a the bounds on the 8 di-scalar channels for the fermiophilic scenario, consisting of third generation quarks plus one additional W boson per doubly charged scalar due to the 3-body decay of $S^{\pm\pm}$. In channels with multiple top quarks, the dominant bounds stem from a search for R-parity violating supersymmetry [60], while various supersymmetric searches [61–64] and the generic search of ref. [65] are relevant for the multi-bottom channels.

Figures 2b to 2d show bounds for various channels of the fermiophobic scenario which are split into three figures for the sake of readability. In Fig. 2b we display di-scalar channels with at least one doubly-charged scalar, leading to at least 3 W bosons plus a W, Z, or photon. The photon channel $WWW\gamma$ can be constrained using measurements of the $Z\gamma$ production cross section [68, 69]. The most relevant searches for the $WWWW$ and $WWWZ$ channels look for multi-lepton final states [57, 70]. For these channels, the results of the ATLAS search [56] apply, and they are shown as blue

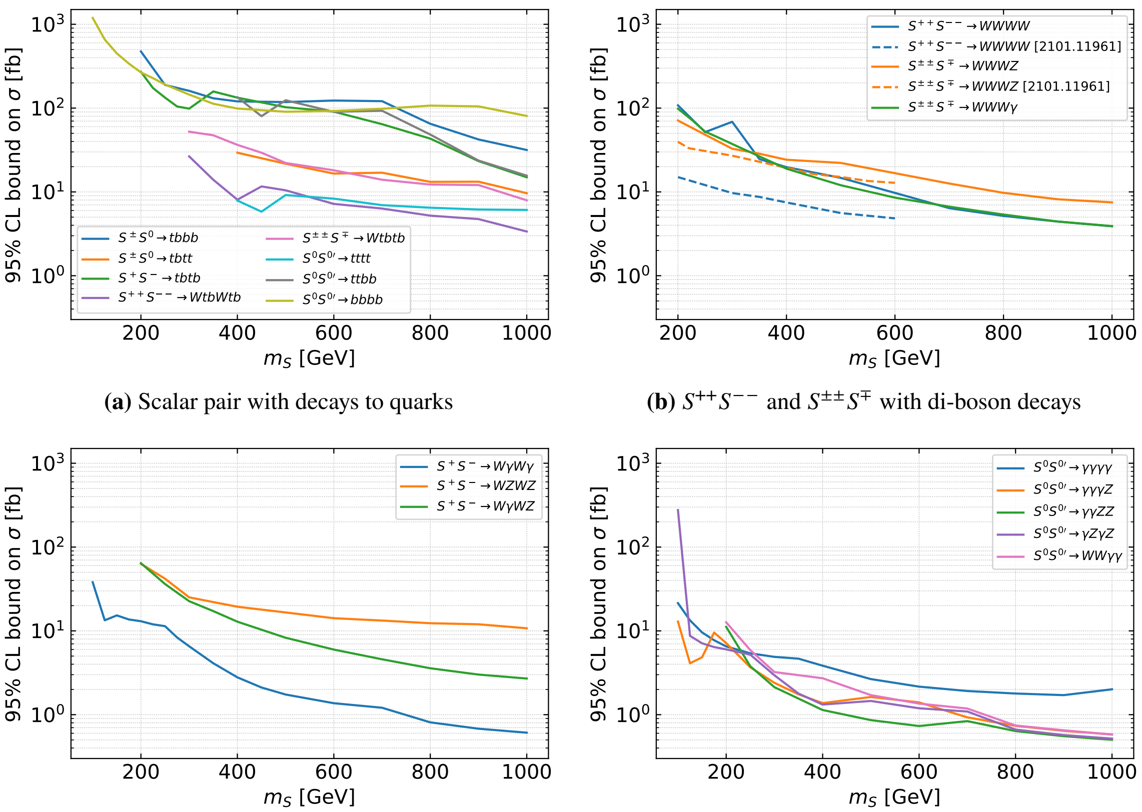

(a) Scalar pair with decays to quarks

(b) $S^{++}S^{--}$ and $S^{\pm\pm}S^{\mp}$ with di-boson decays

(c) S^+S^- with di-boson decays

(d) $S^0 S^{0\prime}$ with di-boson decays with ≥ 2 photons

Figure 2: Upper limits on the cross section of the di-scalar channels from Drell-Yan pair production. The scalars decay to: (a) third generation quarks or (b)-(d) two vector bosons. Both scalars are assumed to have the same mass. The analyses contributing to the bounds are refs. [57–70].

and orange dashed lines. The bounds from this dedicated search are obviously stronger compared the bounds obtained from our recasts of a large number of BSM searches which target different signatures and scenarios. This had to be expected and Figure 2c shows the di-scalar channels from S^+S^- production. We note, that the bounds on $W\gamma W\gamma$ are by far the strongest, stemming from a search for gauge-mediated supersymmetry in final states containing photons and jets [58]. The main bounds for the channels $WZWZ$ and $W\gamma WZ$ stem from a multi-lepton search [65] and the $Z\gamma$ cross section measurements [68, 69], respectively. Finally, in Fig. 2d we present the $S^0S^{0\prime}$ channels containing at least 2 photons. The generic search [62] and the measurement of the $\gamma\gamma$-production cross section [59] constrain the $\gamma\gamma\gamma\gamma$ channel. For the remaining channels, the most important analysis is a (multi-)photon search [58].

3. Bounds on the SU(5)/SO(5) pNGBs

Investigating simplified model is very useful approach as the limits can be applied to a broad class of models, at least to a certain extent. We investigate now a specific full model with an extended EW scalar sector, study the bounds on the full model and compare the results to estimates one can very quickly obtain by using the simplified model approach of the previous section. We take the

SU(5)/SO(5) coset [25] as an example as it features a doubly charged scalar. We first summarise some key elements and discuss some details of the underlying LHC phenomenology. For detailed discussions and the underlying couplings we refer to refs. [26, 27]. The pNGBs of the EW sector form a **14** of SO(5) which decomposes with respect to the custodial $\mathrm{SU}(2)_L \times \mathrm{SU}(2)_R$ as

$$\mathbf{14} \to (\mathbf{3},\mathbf{3}) + (\mathbf{2},\mathbf{2}) + (\mathbf{1},\mathbf{1})\,. \tag{4}$$

We identify the $(\mathbf{2},\mathbf{2})$ with the Higgs doublet. The bi-triplet can be decomposed under the custodial $\mathrm{SU}(2)_D \subset \mathrm{SU}(2)_L \times \mathrm{SU}(2)_R$ as [25]

$$(\mathbf{3},\mathbf{3}) \to \mathbf{1}+\mathbf{3}+\mathbf{5} \equiv \eta_1 + \eta_3 + \eta_5\,, \tag{5}$$

with

$$\eta_1 = \eta_1^0, \quad \eta_3 = (\eta_3^+, \eta_3^0, \eta_3^-), \quad \eta_5 = (\eta_5^{++}, \eta_5^+, \eta_5^0, \eta_5^-, \eta_5^{--}). \tag{6}$$

This basis is suggested by the fact that the vacuum of the strong sector preserves the custodial $\mathrm{SU}(2)_D$. In the following we neglect a possible mixing and assume that the three multiplets have common masses m_1, m_3 and m_5, respectively, to simplify the analysis. Mass differences are due to the EW symmetry breaking, hence one naively expects a relative mass split of the order v/m_i ($i = 1, 3, 5$) with v being the vev of the Higgs boson.

The LHC signatures of pNGB pair production depend strongly on whether the pNGBs are fermiophilic or fermiophobic as already mentioned above. We start with a brief discussion of the fermiophobic case and refer to ref. [27] for further details. The singly charged states decay as

$$\eta_{3,5}^+ \to W^+\gamma,\; W^+Z\,, \tag{7}$$

with dominant photon channel as $\mathrm{Br}(\eta_{3,5}^+ \to W^+\gamma) \approx \cos^2\theta_W \approx 78\%$ [25] for both multiplets in case of a small mass split between the multiplets. The neutral singlet and quintuplet decay dominantly as

$$\eta_{1,5}^0 \to \gamma\gamma,\; \gamma Z,\; ZZ\,, \tag{8}$$

with comparable branching ratios, again for small mass split. The only available decay channel for the doubly charged pNGB in the quintuplet is

$$\eta_5^{++} \to W^+W^+. \tag{9}$$

Finally, the η_3^0 is CP-even and thus undergoes three-body decays via off-shell pNGBs:

$$\eta_3^0 \to W^+W^-\gamma,\; W^+W^-Z \quad \text{via } \eta_{3,5}^{\pm(*)}\,, \text{ and} \tag{10a}$$

$$\eta_3^0 \to Z\gamma\gamma,\; ZZ\gamma,\; ZZZ \qquad \text{via } \eta_{1,5}^{0(*)}\,. \tag{10b}$$

The discussion so far applies to the lightest multiplet and also covers scenarios where the multiplets are very close in mass. However, there could be a sizeable mass split. In such a case, cascade decays from one multiplet into a lighter one and a (potentially off-shell) vector boson become important. Taking the case $m_5 > m_3 > m_1$ as an example, we have

$$\eta_5^{++} \to W^{+(*)}\eta_3^+, \qquad \eta_5^+ \to Z^{(*)}\eta_3^+,\; W^{+(*)}\eta_3^0, \qquad \eta_5^0 \to W^{\pm(*)}\eta_3^\mp,\; Z^{(*)}\eta_3^0, \tag{11a}$$

$$\eta_3^+ \to W^{+(*)}\eta_1^0, \qquad \eta_3^0 \to Z^{(*)}\eta_1^0. \tag{11b}$$

One finds that both classes of decays are of similar importance once the mass split is between 30 and 50 GeV [27]. We note for completeness, that the η_5 multiplet does not couple to η_1^0 in the model considered.

One expects in the fermiophilic case that the couplings scale like the quark masses, e.g.

$$\kappa_t^{\eta_i^0} = c_t^i \frac{m_t}{f} \quad , \quad \kappa_b^{\eta_i^0} = c_b^i \frac{m_b}{f} \quad \text{and} \quad \kappa_{tb}^{\eta_j^+} = c_{tb}^j \frac{m_t}{f} \,, \tag{12}$$

where f is the decay constant of the **14**-plet and the c coefficients are of order one. In this case the decays to third generation quarks dominate over the loop-level anomaly-induced decays into two vector bosons or the three-body decays discussed above and, thus, we consider the decays

$$\eta_{3,5}^+ \to t\bar{b}, \qquad \eta_{1,3,5}^0 \to t\bar{t},\, b\bar{b}\,. \tag{13}$$

From Eq. (12), the $t\bar{t}$ channel dominates over $b\bar{b}$ above threshold. In the case of η_5^{++}, the three-body decay

$$\eta_5^{++} \to W^+ t\bar{b} \tag{14}$$

via an off-shell $\eta_{3,5}^+$ dominantes over the decay to W^+W^+. In case of $m_5 > m_3$ also the decay $\eta_5^{++} \to W^{+(*)}\eta_3^+$ becomes important [27].

We consider in a first step only the quintuplet η_5 and apply the simplified model bounds from the previous section. In Fig. 3a we compare the cross section times branching ratio of all multi-photon final states (solid lines) with the corresponding bounds from Fig. 2 (dashed lines). From the individual channels one finds that masses below 340 GeV are excluded, with the strongest bound coming from the channel $\eta_5^\pm\eta_5^0 \to W\gamma\gamma\gamma$. We perform in addition a full simulation in which all states contained in the quintuplet are pair-produced and decayed. The solid green line denotes the sum over all pair production cross sections of the quintuplet and the dashed green line the corresponding bound, i.e. the sum of scalar pair production cross sections that would be needed in order to exclude the convolution of all decay channels from quintuplet states. As can be seen, one obtains a bound of 485 GeV on the mass m_S which is significantly higher than the bounds obtained from individual channels. The apparent discrepancy between simplified models and the full simulation can be understood from the fact that all multi-photon channels populate the same signal region of the search presented in ref. [58]. Adding up the various signal cross sections with two or more photons gives the blue line in Fig. 3b. This summed cross section yields an estimated bound on m_S of $460 - 500$ GeV when compared with the bounds from different multi-photon channels (shaded area in Fig. 3b). This is in agreement with the result of the full simulation. This example shows the usefulness and limitations of the simplified model bounds and demonstrate how they can be combined in the context of a particular model.

In a second step, we take all multiplets into account and consider two scenarios which are characterised by varying a single mass scale m_S:

$$\text{S-eq:} \quad m_3 = m_S - 2\text{ GeV}, \qquad m_5 = m_S, \quad m_1 = m_S + 2\text{ GeV}\,; \tag{15a}$$

$$\text{S-135:} \quad m_1 = m_S - 50\text{ GeV}, \quad m_3 = m_S, \quad m_5 = m_S + 50\text{ GeV}\,. \tag{15b}$$

The choice of 50 GeV is motivated by the fact that the mass splits are expected to be a fraction of the Higgs vev. The phenomenology differs in the two cases: In scenario S-eq, all particles decay via

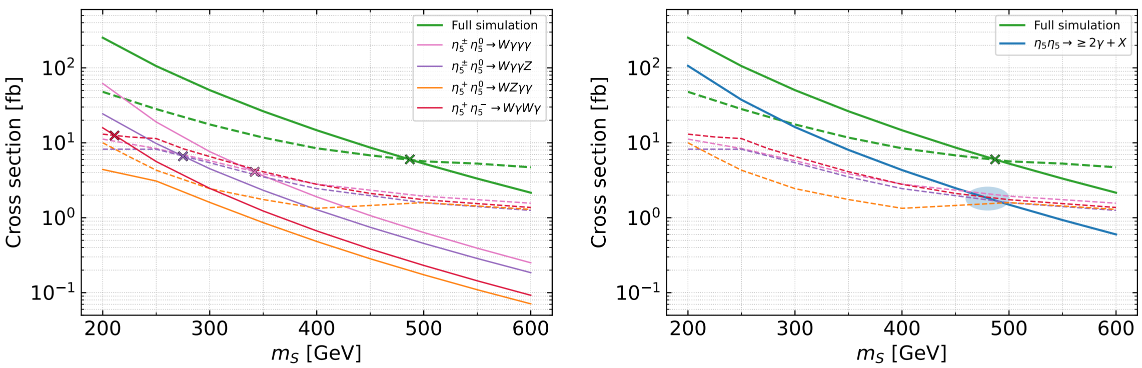

(a) Bounds from individual channels **(b)** Bounds from sum of multiphoton channels

Figure 3: Application of the model-independent bounds to a specific model, the custodial quintuplet η_5 from the $\mathrm{SU}(5)/\mathrm{SO}(5)$ coset. In (a) we determine the bounds from the dominant individual channels by comparing the cross section time branching ratio from the model (solid) with the upper limits from Fig. 2 (dashed). In green we show the results of a full simulation. The blue line in (b) is the sum of the individual multi-photon cross sections shown in (a). Further details are given in the text.

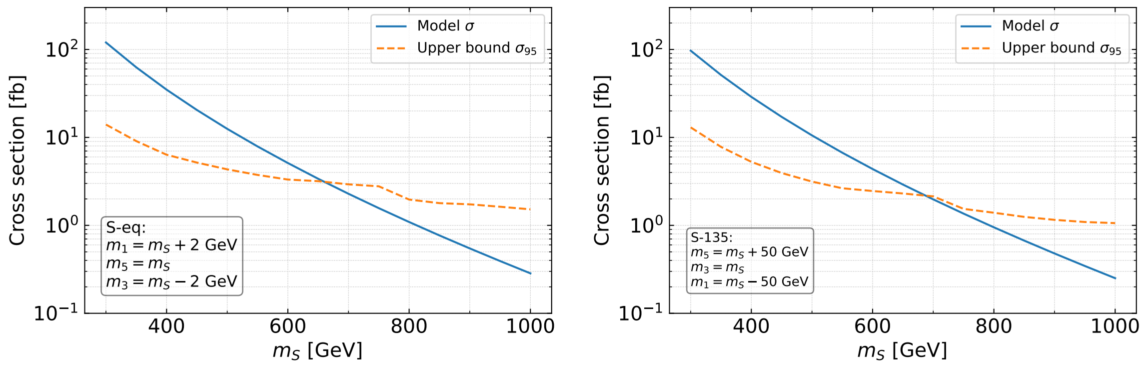

(a) Scenario S-eq **(b)** Scenario S-135

Figure 4: Bounds on the pNGB masses for the Drell-Yan production of the full bi-triplet for the benchmark mass spectra defined in Eq. (15). In (a) all masses are approximately equal and in (b) there is a 50 GeV mass split between the multiplets.

the anomaly and η_3^0 exhibits three-body decays. We introduce a small mass split of 2 GeV to avoid a cancellation for some η_3^0 decays as discussed in ref. [27]. In scenario S-135 the heavier states decay into the next lighter states or di-bosons, while the lightest state only has anomaly induced decays. We present the bounds on the mass parameter m_S for the two scenarios in Fig. 4. In orange the sums over all scalar pair production cross sections σ_{95} is shown that would be needed to exclude the model at 95% CL at each parameter point. The strongest bounds come from multi-photon channels, with ref. [58] being the dominant analysis. Note, that the kink in σ_{95} is due to a change in dominant signal region within the same analysis. In blue, the actual sum over all pair production cross sections in this model is drawn. The different bounds for these scenarios considered are due to the relative size of the cross section for the triplet and quintuplet.

We turn now to the scenarios in which the pNGBs couple dominantly to quarks. In these

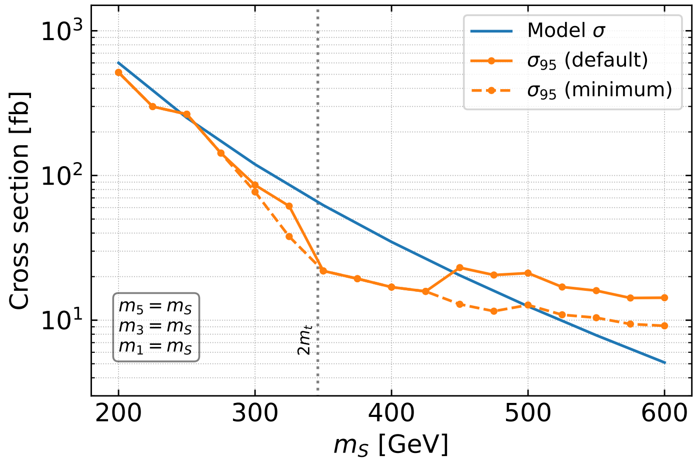

Figure 5: Bounds on the pNGB masses for the Drell-Yan production of the full bitriplet with decays to third-generation quarks.

scenarios, one has single scalar production via the processes

$$pp \to S^0 t\bar{t} \quad \text{and} \quad pp \to S^{\pm} tb \tag{16}$$

induced by strong interactions. In addition, the couplings of the neutral scalars to quarks induce couplings to gluons and photons at the one-loop level leading to processes like

$$pp \to S^0 \to t\bar{t} \quad \text{and} \quad pp \to S^0 \to \gamma\gamma\,. \tag{17}$$

It turns out that presently available searches can constrain these channels for masses of up to 500 GeV only if the c-factors in Eq. (12) are close to 5 and a decay constant f of 1 TeV which is only a very small part of the available parameter space.

We now turn to Drell-Yan pair production and display our results in Fig. 5. We have assumed that all pNGBs are mass degenerate and that all c-factors are 1. Note, that neither branching ratios nor production cross sections depend on f. The blue line gives the total cross section summing over all pNGBs irrespective of their decay modes. The orange lines give the exclusion when considering all possible channels. The exclusion is dominated by the results of ref. [60] implemented in CheckMATE. CheckMATE uses the signal region with the strongest expected bound and reports the corresponding observed bound as final result. One obtains the bound given by the solid orange line using this standard procedure. This can lead to difficulties in cases for which observed and expected bounds differ significantly. This is the reason for the kinks at $m_S = 350$ GeV and 450 GeV. However, modifying the procedure such that always the strongest observed bound is taken, one obtains a smoother curve shown by the dashed orange line, see [27] for further details.

We note for completeness, that models with and gauge/fermionic underlying dynamics [10, 28, 29] also predict pNGBs which are strongly interacting. The $SU(5)/SO(5)$ coset is for example realized in the model M5 of ref. [30] which predicts beside the electroweak pNGBs discussed above also a color triplet pNGB π_3 and a color octet pNGB π_8. The π_8 decays either dominantly into tt or gg depending on whether we are in a fermiophilic or a fermiophobic scenarios, respectively. In both cases currently available analyses give a bound of about 1.1 TeV on its mass [71]. The π_3 has the same quantum numbers as a right-handed stop, the supersymmetric partner of the right-handed top-quark, and its phenomenology depends on the mass spectrum of the baryonic bound states [72]. This baryonic bound states contain two color neutral fermions denoted by $\tilde{b}$ and $\tilde{h}$ in [72] where the first one is a gauge singlet and the second an $SU(2)_L$ doublet with hypercharge 1/2. It is possible that this states, being color singlets, can be lighter than π_3. In such a scenario the π_3 decays into one of these fermions and an SM-fermion:

$$\pi_3 \to t\tilde{B},\ t\tilde{h}^0,\ b\tilde{h}^+ . \tag{18}$$

This resembles the decays of stops in supersymmetric models. In principle, decays into lighter families, like $c\,\tilde{B}$ and $u\,\tilde{B}$, are also possible, but in the spirit of composite Higgs models we expect those to be strongly suppressed. Consequently, LHC bounds from stop searches can be directly applied [73–75]. For large mass differences this gives a bound of about 1.3 TeV. We note fore completeness, that in case of small mass difference between π_3 and $\tilde{B}$ three-body decays via an off-shell top-quark would become important similar to supersymmetric models [76–78]. In case that π_3 is lighter than these baryons, lepton or baryon number violating interactions need to be included in order to avoid a stable π_3 which require an extension of this model [72]. The simplest possibilities are

$$\pi_3 \to \bar{d}_i\,\bar{d}_j \qquad \text{with } d_i = d, s, b \text{ and } i \neq j \tag{19}$$

or

$$\pi_3 \to u_i\,\nu_{l_j}\,,\ d_i\,l_j \qquad \text{with } u_i = u, c, t \text{ and } l_j = e, \mu, \tau\,. \tag{20}$$

The former violates baryon number whereas the latter violates lepton number. Note, that only one of the two interaction types can be present as otherwise the proton could decay at a rate incompatible with experiment. In case of lepton number violation, one can use searches for leptoquarks and finds a bound of 1.4-1.5 TeV depending on whether final states with a τ or e, μ dominates [79, 80].

4. Conclusions

In this contribution we have presented bounds on the Drell-Yan pair production of scalar bosons that carry electroweak charges at the LHC. We first consider various channels in a simplified model approach. These channels contain either four vector bosons or top/bottom quarks in the final states. These two scenarios arise from fermiophobic and fermiophilic models, respectively. The limits, presented in Fig. 2, can be applied to any model with an extended Higgs sector dominated by pair production.

In addition we have taken as a concrete example a composite Higgs model based on the coset SU(5)/SO(5), which features a custodial bi-triplet. We show that while the limits on individual channels lead to relatively weak bounds on the scalar masses, significantly stronger bounds can be obtained by combining various pair production channels. Considering various benchmark scenarios, limits on the scalar mass scale around 500 – 700 GeV have been established in the fermiophobic case. The bounds are close to 500 GeV in scenarios in which decays into top and bottom quarks dominate.

PoS(CORFU2022)126

Acknowlegments

I thank the organizers of this meeting for an inspiring atmosphere. I also thank J. Butterworth, G. Cacciapaglia, T. Flacke, M. Kunkel, R. Ströhmer and L. Schwarze for discussions.

References

[1] F. Englert and R. Brout, Phys. Rev. Lett. **13** (1964), 321-323.

[2] P. W. Higgs, Phys. Rev. Lett. **13** (1964), 508-509.

[3] G. Aad *et al.* [ATLAS], Phys. Lett. B **716** (2012), 1-29 [arXiv:1207.7214 [hep-ex]].

[4] S. Chatrchyan *et al.* [CMS], Phys. Lett. B **716** (2012), 30-61 [arXiv:1207.7235 [hep-ex]].

[5] S. P. Martin, Adv. Ser. Direct. High Energy Phys. **18** (1998), 1-98 [arXiv:hep-ph/9709356 [hep-ph]].

[6] G. C. Branco *et al.*, Phys. Rept. **516** (2012), 1-102 [arXiv:1106.0034 [hep-ph]].

[7] J. Schechter and J. W. F. Valle, Phys. Rev. D **22** (1980), 2227.

[8] M. Hirsch, S. Kaneko and W. Porod, Phys. Rev. D **78** (2008), 093004 [arXiv:0806.3361 [hep-ph]].

[9] H. Georgi and M. Machacek, Nucl. Phys. B **262** (1985), 463-477.

[10] G. Ferretti, JHEP **06** (2016), 107 [arXiv:1604.06467 [hep-ph]].

[11] D. B. Kaplan and H. Georgi, Phys. Lett. B **136** (1984), 183-186.

[12] S. Weinberg, Phys. Rev. D **13** (1976), 974-996.

[13] S. Dimopoulos and L. Susskind, Nucl. Phys. B **155** (1979), 237-252.

[14] K. Agashe, R. Contino and A. Pomarol, Nucl. Phys. B **719** (2005), 165-187 [arXiv:hep-ph/0412089 [hep-ph]].

[15] E. Witten, Nucl. Phys. B **223** (1983), 422-432.

[16] D. A. Kosower, Phys. Lett. B **144** (1984), 215-216.

[17] H. Georgi and D. B. Kaplan, Phys. Lett. B **145** (1984), 216-220.

[18] K. Agashe *et al.*, Phys. Lett. B **641** (2006), 62-66 [arXiv:hep-ph/0605341 [hep-ph]].

[19] T. A. Ryttov and F. Sannino, Phys. Rev. D **78** (2008), 115010 [arXiv:0809.0713 [hep-ph]].

[20] J. Galloway *et al.*, JHEP **10** (2010), 086 [arXiv:1001.1361 [hep-ph]].

[21] M. J. Dugan, H. Georgi and D. B. Kaplan, Nucl. Phys. B **254** (1985), 299-326.

[22] N. Arkani-Hamed *et al.*, JHEP **07** (2002), 034 [arXiv:hep-ph/0206021 [hep-ph]].

[23] T. Ma and G. Cacciapaglia, JHEP **03** (2016), 211 [arXiv:1508.07014 [hep-ph]].

[24] L. Vecchi, JHEP **02** (2017), 094 [arXiv:1506.00623 [hep-ph]].

[25] A. Agugliaro *et al.*, JHEP **02** (2019), 089 [arXiv:1808.10175 [hep-ph]].

[26] A. Banerjee *et al.*, [arXiv:2203.07270 [hep-ph]].

[27] G. Cacciapaglia *et al.*, JHEP **12** (2022), 087 [arXiv:2210.01826 [hep-ph]].

[28] G. Ferretti and D. Karateev, JHEP **03** (2014), 077 [arXiv:1312.5330 [hep-ph]].

[29] G. Ferretti, JHEP **06** (2014), 142 [arXiv:1404.7137 [hep-ph]].

[30] A. Belyaev *et al.*, JHEP **01** (2017), 094 [erratum: JHEP **12** (2017), 088] [arXiv:1610.06591 [hep-ph]].

[31] E. Bennett *et al.*, JHEP **03** (2018), 185 [arXiv:1712.04220 [hep-lat]].

[32] E. Bennett *et al.*, JHEP **12** (2019), 053 [arXiv:1909.12662 [hep-lat]].

[33] E. Bennett *et al.*, Phys. Rev. D **101** (2020) no.7, 074516 [arXiv:1912.06505 [hep-lat]].

[34] E. Bennett *et al.*, Phys. Rev. D **106** (2022) no.9, 094503 [arXiv:2205.09364 [hep-lat]].

[35] J. Erdmenger *et al.*, Phys. Rev. Lett. **126** (2021) no.7, 071602 [arXiv:2009.10737 [hep-ph]].

[36] J. Erdmenger *et al.*, JHEP **02** (2021), 058 [arXiv:2010.10279 [hep-ph]].

[37] J. Erdmenger, Y. Liu, N. Evans and W. Porod, in preparation.

[38] A. Alloul *et al.*, Comput. Phys. Commun. **185** (2014), 2250-2300 [arXiv:1310.1921 [hep-ph]].

[39] J. Alwall *et al.*, JHEP **07** (2014), 079 [arXiv:1405.0301 [hep-ph]].

[40] R. D. Ball *et al.*, Nucl. Phys. B **867** (2013), 244-289 [arXiv:1207.1303 [hep-ph]].

[41] A. Buckley *et al.*, Eur. Phys. J. C **75** (2015), 132 [arXiv:1412.7420 [hep-ph]].

[42] T. Sjöstrand *et al.*, Comput. Phys. Commun. **191** (2015), 159-177 [arXiv:1410.3012 [hep-ph]].

[43] E. Conte, B. Fuks and G. Serret, Comput. Phys. Commun. **184** (2013), 222-256 [arXiv:1206.1599 [hep-ph]].

[44] E. Conte *et al.*, Eur. Phys. J. C **74** (2014) no.10, 3103 [arXiv:1405.3982 [hep-ph]].

[45] B. Dumont *et al.*, Eur. Phys. J. C **75** (2015) no.2, 56 [arXiv:1407.3278 [hep-ph]].

[46] E. Conte and B. Fuks, Int. J. Mod. Phys. A **33** (2018) no.28, 1830027 [arXiv:1808.00480 [hep-ph]].

[47] M. Drees *et al.*, Comput. Phys. Commun. **187** (2015), 227-265 [arXiv:1312.2591 [hep-ph]].

[48] D. Dercks *et al.*, Comput. Phys. Commun. **221** (2017), 383-418 [arXiv:1611.09856 [hep-ph]].

[49] J. de Favereau *et al.* [DELPHES 3], JHEP **02** (2014), 057 [arXiv:1307.6346 [hep-ex]].

[50] M. Cacciari, G. P. Salam and G. Soyez, JHEP **04** (2008), 063 [arXiv:0802.1189 [hep-ph]].

[51] M. Cacciari, G. P. Salam and G. Soyez, Eur. Phys. J. C **72** (2012), 1896 [arXiv:1111.6097 [hep-ph]].

[52] A. L. Read, J. Phys. G **28** (2002), 2693-2704

[53] C. Bierlich *et al.*, SciPost Phys. **8** (2020), 026 [arXiv:1912.05451 [hep-ph]].

[54] J. M. Butterworth *et al.*, JHEP **03** (2017), 078 [arXiv:1606.05296 [hep-ph]].

[55] A. Buckley *et al.*, SciPost Phys. Core **4** (2021), 013 [arXiv:2102.04377 [hep-ph]].

[56] G. Aad *et al.* [ATLAS], JHEP **06** (2021), 146 [arXiv:2101.11961 [hep-ex]].

[57] CMS Collaboration, CMS-PAS-EXO-19-002.

[58] M. Aaboud *et al.* [ATLAS], Phys. Rev. D **97** (2018), 092006 [arXiv:1802.03158 [hep-ex]].

[59] G. Aad *et al.* [ATLAS], JHEP **11** (2021), 169 [arXiv:2107.09330 [hep-ex]].

[60] G. Aad *et al.* [ATLAS], Eur. Phys. J. C **81** (2021) no.11, 1023 [arXiv:2106.09609 [hep-ex]].

[61] G. Aad *et al.* [ATLAS], Eur. Phys. J. C **81** (2021) no.7, 600 [erratum: Eur. Phys. J. C **81** (2021) no.10, 956] [arXiv:2101.01629 [hep-ex]].

[62] M. Aaboud *et al.* [ATLAS], Eur. Phys. J. C **79** (2019) no.2, 120 [arXiv:1807.07447 [hep-ex]].

[63] G. Aad *et al.* [ATLAS], JHEP **12** (2019), 060 [arXiv:1908.03122 [hep-ex]].

[64] CMS Collaboration, CMS-PAS-SUS-19-006.

[65] A. M. Sirunyan *et al.* [CMS], Phys. Rev. D **96** (2017), 032003 [arXiv:1704.07781 [hep-ex]].

[66] G. Aad *et al.* [ATLAS], JHEP **10** (2020), 005 [arXiv:2004.10894 [hep-ex]].

[67] G. Aad *et al.* [ATLAS], JHEP **07** (2021), 005 [arXiv:2103.01918 [hep-ex]].

[68] G. Aad *et al.* [ATLAS], JHEP **03** (2020), 054 [arXiv:1911.04813 [hep-ex]].

[69] M. Aaboud *et al.* [ATLAS], JHEP **12** (2018), 010 [arXiv:1810.04995 [hep-ex]].

[70] A. M. Sirunyan *et al.* [CMS], JHEP **03** (2018), 166 [arXiv:1709.05406 [hep-ex]].

[71] G. Cacciapaglia *et al.*, JHEP **11** (2015), 201 [arXiv:1507.02283 [hep-ph]].

[72] G. Cacciapaglia *et al.*, JHEP **02** (2022), 208 [arXiv:2112.00019 [hep-ph]].

[73] A. M. Sirunyan *et al.* [CMS], JHEP **10** (2019), 244 [arXiv:1908.04722 [hep-ex]].

[74] G. Aad *et al.* [ATLAS], JHEP **04** (2021), 174 [arXiv:2012.03799 [hep-ex]].

[75] A. Tumasyan *et al.* [CMS], Eur. Phys. J. C **81** (2021) no.11, 970 [arXiv:2107.10892 [hep-ex]].

[76] W. Porod and T. Wöhrmann, Phys. Rev. D **55** (1997), 2907-2917 [erratum: Phys. Rev. D **67** (2003), 059902] [arXiv:hep-ph/9608472 [hep-ph]].

[77] W. Porod, Phys. Rev. D **59** (1999), 095009 [arXiv:hep-ph/9812230 [hep-ph]].

[78] C. Boehm, A. Djouadi and Y. Mambrini, Phys. Rev. D **61** (2000), 095006 [arXiv:hep-ph/9907428 [hep-ph]].

[79] ATLAS collaboration, [arXiv:2210.04517 [hep-ex]].

[80] ATLAS collaboration, [arXiv:2303.01294 [hep-ex]].